Biochemical and Biophysical Research Communications 619 (2022) 117–123

Contents lists available at ScienceDirect

Biochemical and Biophysical Research Communications

journal homepage: www.elsevier.com/locate/ybbrc

YAP1/TAZ activity maintains vascular integrity and organismal survival

Shun Uemura [a, c], Masayuki Yamashita [a], Kazumasa Aoyama [a], Takako Yokomizo-Nakano [a], Motohiko Oshima [a], Miki Nishio [d], Masayoshi Masuko [c], Jun Takizawa [c], Hirohito Sone [c], Yasuhiro Yamada [b], Akira Suzuki [d], Atsushi Iwama [a, e, *]

[a] Division of Stem Cell and Molecular Medicine, Center for Stem Cell Biology and Regenerative Medicine, The Institute of Medical Science, The University of Tokyo, Tokyo, Japan
[b] Division of Stem Cell Pathology, Center for Experimental Medicine and Systems Biology, The Institute of Medical Science, The University of Tokyo, Tokyo, Japan
[c] Department of Hematology, Endocrinology, and Metabolism, Niigata University Faculty of Medicine, Niigata, Japan
[d] Division of Molecular and Cellular Biology, Kobe University Graduate School of Medicine, Kobe, Japan
[e] Laboratory of Cellular and Molecular Chemistry, Graduate School of Pharmaceutical Sciences, The University of Tokyo, Tokyo, Japan

ARTICLE INFO

Article history:
Received 23 May 2022
Accepted 15 June 2022
Available online 19 June 2022

Keywords:
Yes-associated protein 1 (YAP1)
WW domain Containing transcription regulator 1 (TAZ)
Endothelial cell
Ionizing radiation
Lung
Tight junction

ABSTRACT

Radiation therapy is one of the major treatment modalities for patients with cancers. However, ionizing radiation (IR) damages not only cancer cells but also the surrounding vascular endothelial cells (ECs). Hippo pathway effector genes *Yap1* and *Taz* are the two transcriptional coactivators that have crucial roles in tissue homeostasis and vascular integrity in various organs. However, their function in adult ECs at the steady state and after IR is poorly understood. Here, we report sex- and context-dependent roles of endothelial YAP1/TAZ in maintaining vascular integrity and organismal survival. EC-specific *Yap1/Taz* deletion compromised systemic vascular integrity, resulting in lethal circulation failure preferentially in male mice. Furthermore, EC-specific *Yap1/Taz* deletion induced acute lethality upon sublethal IR that was closely associated with exacerbated systemic vascular dysfunction and circulation failure. Consistent with these findings, RNA-seq analysis revealed downregulation of tight junction genes in *Yap1/Taz*-deleted ECs. Collectively, our findings highlight the importance of endothelial YAP1/TAZ for maintaining adult vascular function, which may provide clinical implications for preventing organ injury after radiation therapy.

1. Introduction

Ionizing radiation (IR) eliminates cancer cells via apoptosis by inducing DNA damage and oxidative stress. By utilizing this biological effect, radiation therapy (RT) is one of the major and established therapeutic options for patients with various types of cancer. Despite the advance in radiation technologies and the advent of multimodal radiotherapy, radiation-induced tissue damage remains a serious concern due to the cytotoxic effect of IR on the surrounding intact tissues [1]. Vascular endothelial cells (ECs) are sensitive to IR, as demonstrated by IR-induced alteration in vascular structure and function [1,2]. This endothelial IR sensitivity seems of clinical importance, as cardiovascular complication in chest radiation therapy for mediastinal Hodgkin lymphoma [3] and increased risk of cardiovascular diseases in atomic bomb survivors and nuclear industry workers [4,5] have been reported. However, the mechanism by which IR causes vascular endothelial damage is not well understood.

The Hippo signaling pathway is an evolutionarily conserved regulator of organ size and tissue regeneration [6,7]. The Hippo signaling negatively regulates the two effector proteins, Yes associated protein 1 (YAP1) and its paralog WW domain containing transcription regulator 1 (TAZ), which promote transactivation of various target genes important for cell proliferation, apoptosis, and stem cell self-renewal, thereby playing indispensable roles in normal tissue development [6,8,9] and regeneration [6], as well as

* Corresponding author. Division of Stem Cell and Molecular Medicine, Center for Stem Cell Biology and Regenerative Medicine, The Institute of Medical Science, The University of Tokyo, 4-6-1 Shirokanedai, Minato-ku, Tokyo, 108-8639, Japan.
E-mail address: 03aiwama@ims.u-tokyo.ac.jp (A. Iwama).

https://doi.org/10.1016/j.bbrc.2022.06.050
0006-291X/

tumorigenesis [10–13]. Cumulative evidence shows that vascular endothelial YAP1/TAZ play a critical role during developmental angiogenesis [14–22], for instance by regulating vascular tip cell formation via CDC42 [23] and modulating VEGF and NOTCH signaling [15,21,24–26]. While YAP1/TAZ in adult ECs are reportedly dispensable for vascular integrity in the steady state [16], they are critical in some pathological contexts such as retinal neovascular formation in diabetes mellitus, age-related macular degeneration models [27–29], and tumor vascularization [14,19,21]. Moreover, the activity of YAP1/TAZ can be differentially regulated by sex hormone receptors [30,31]. However, differential effects of endothelial YAP1/TAZ between males and females or their function in IR-induced vascular changes remain largely uninvestigated.

Here, we investigated the function of YAP1/TAZ in vascular ECs during homeostasis and after acute IR damage. By analyzing EC-specific *Yap1/Taz* deletion mutant mice, we demonstrate sex- and context-dependent roles of YAP1/TAZ in vascular integrity and organismal survival.

2. Materials and methods

2.1. Mice

8-week-old C57Bl/6J mice were purchased from Japan SLC (Shizuoka, Japan). For conditional deletion of *Yap1/Taz*, we bred $Yap1^{fl/fl}$ [32] and $Taz^{fl/fl}$ (kindly provided by J. Wrana) mutants to Cdh5-CreER^{T2} transgenic mice [33] (kindly provided by Y. Kubota) to generate $Cdh5\text{-}CreER^{T2}(+)$; $Yap1^{fl/fl}$; $Taz^{fl/fl}$ mice. To generate endothelial-specific *Yap1/Taz* double knockout mice ($Yap1/Taz^{i\Delta EC}$), 8-week-old $Yap1/Taz^{fl/fl}$ mice were injected intraperitoneally with 100 μl tamoxifen dissolved in corn oil at a concentration of 10 mg/ml for five consecutive days. $Yap1/Taz^{i\Delta EC}$ mice were analyzed 4–5 weeks after the last tamoxifen injection unless otherwise stated. For sublethal irradiation, mice were irradiated with a single dose of 5 Gy using an X-ray irradiator (MBR-1520R-4, HITACHI, Tokyo, Japan). All experiments using mice were performed following our institutional guidelines for the use of laboratory animals and approved by the Review Board for Animal Experiments of The Institute of Medical Science, The University of Tokyo (approval ID: PS18-02). The primer sequences and probes used for genotyping PCR are shown in Supplementary Table 1.

2.2. Flow cytometry analysis and sorting of lung endothelial cells

After isolation, the lung was cut into small pieces with scissors and incubated in 4 mg/mL of collagenase type I (LS004194, Worthington, Columbus, OH, USA) in Dulbecco's Modified Eagle Medium (D5796, Sigma-Aldrich, St. Louis, MO, USA) at 37 °C with mild shaking. After hemolysis with ammonium-chloride-potassium (ACK) lysing buffer, cells were stained with monoclonal antibodies recognizing the following antigens: CD45 (30F11; BD Biosciences, Franklin Lakes, NJ, USA), PDGFRα (APA5; BioLegend), Sca-1 (D7; BioLegend, San Diego, CA, USA), CD31 (390; BioLegend), and Ter119 (TER-119; Thermo Fisher Scientific, Waltham, MA, USA). Dead cells were removed by staining with 0.5 μg/ml propidium iodide (Sigma-Aldrich). All flow cytometric analyses and cell sorting were performed on FACSAria IIIu (BD Bioscience).

2.3. Quantitative RT-PCR

Total RNA was extracted using RNeasy Mini Kit (QIAGEN, Hilden, Germany) and reverse transcribed by SuperScript III First-Strand Synthesis System (Invitrogen, Waltham, MA, USA). Real-time quantitative PCR was performed with StepOnePlus Real-Time PCR System (Life Technologies, Waltham, MA, USA) using TB Green Premix Ex Taq II (Takara Bio). All data are presented as relative expression levels normalized to *Hprt* expression. The primer sequences and probes used are shown in Supplementary Table 2.

2.4. Micro-CT

After the mice were anesthetized with isoflurane, micro-CT scanning was performed using a CosmoScan R-mCT2 (Rigaku, Tokyo, Japan). Horos Viewer (Horos project, https://horosproject.org/) was used for editing images and measuring cardio-thoracic ratio (CTR).

2.5. Histological analysis

Organs and tissues were fixed with formalin and subjected to histological analysis. Organ and tissue sections were stained with Hematoxylin and Eosin (H&E).

2.6. RNA-sequence analysis

Total RNA was extracted from 10,000 cells using RNeasy Plus Micro Kit (QIAGEN), and cDNA was synthesized using SMART-Seq v4 Ultra Low Input RNA Kit for Sequencing (TaKaRa bio, Shiga, Japan) according to the manufacturer's instructions. The double-stranded cDNA was fragmented using S220 Focused-ultrasonicator (Covaris, Woburn, MA, USA), then cDNA libraries were generated using NEBNext Ultra DNA Library Prep Kit (New England BioLabs, Ipswich, MA, USA) according to the manufacturer's instructions. Sequencing was performed using HiSeq2500 (Illumina, San Diego, CA, USA) with a single-read sequencing length of 60bp. Sequencing quality control was performed using FastQC (http://www.bioinformatics.babraham.ac.uk/projects/fastqc/). TopHat (version 2.0.13; with default parameters) was used to map the reads to the reference genome (UCSC/mm10) with annotation data from iGenomes (Illumina), and transcript per million (TPM) for each gene was quantified using Cuffdiff (Cufflinks version 2.2.1; with default parameters) using the super-computing resource provided by the Human Genome Center of our institute (http://sc.hgc.jp/shirokane.html). A PCA plot was generated based on expression of all genes. Differentially expressed genes were identified using FDR <0.05. Kyoto Encyclopedia of Genes and Genomes (KEGG) pathway analysis was performed using g:Profiler (https://biit.cs.ut.ee/gprofiler/) and gene set enrichment analysis (GSEA) [34] using the YAP conserved signature gene [35] and KEGG tight junction signature gene (https://www.genome.jp/kegg/pathway/hsa/hsa04530.html). Differential gene expression was determined using the edgeR [36]. Heatmaps showing z-score of transcripts per million (TPM) for YAP1/TAZ targets and tight junction-related genes were generated with hierarchical clustering of samples with Morpheus (https://software.broadinstitute.org/morpheus).

2.7. Statistical analysis

Two groups were compared using the unpaired two-tailed Student's *t*-test. Data are shown as means ± SD. Survival curve was obtained using the Kaplan-Meier method, and statistical differences were analyzed using the log-rank test. Significance was indicated by *p < 0.05, **p < 0.01, ***p < 0.001, ****p < 0.0001 and n.s. (not significant). All statistical analysis was performed using GraphPad Prism 9 (GraphPad Software, San Diego, CA, USA).

2.8. Data availability

RNA sequence data were deposited in the DDBJ (accession number PRJDB13628).

3. Results

3.1. Endothelial-specific deletion of Yap1/Taz causes lethality in adult male mice

To understand the physiological role of YAP1/TAZ in adult vascular ECs, we utilized *Cdh5-CreER^{T2}; Yap1$^{fl/fl}$; Taz$^{fl/fl}$* mice [34]. To conditionally delete *Yap1/Taz* genes in vascular ECs, we intraperitoneally injected the mice with tamoxifen (1.0 mg/mice, 5 consecutive days) (Fig. 1A). We confirmed the efficient deletion of *Yap1/Taz* in lung vascular ECs by quantitative RT-PCR at 4 weeks post-tamoxifen treatment (Fig. 1B). Genomic PCR of lung vascular ECs demonstrated that *Yap1/Taz* were deleted in lung ECs but not in tail genomic DNA from Cre-positive mice (Supplementary Fig. S1A), confirming ECs-specific deletion of *Yap1/Taz* (*Yap1/Taz$^{i\Delta EC}$*) in our model.

To evaluate the impact of *Yap1/Taz* deletion in adult ECs during the steady state, we evaluated the survival of control and mutant mice after tamoxifen injection. Unexpectedly, male *Yap1/Taz$^{i\Delta EC}$* mice showed significantly shorter survival after tamoxifen treatment (Median survival = 125.0 days) (Fig. 1C). In contrast, only 1 out of 5 female *Yap1/Taz$^{i\Delta E}$* mice show lethal phenotype and most of them survived post-tamoxifen injection. These results suggest that EC-specific deletion of *Yap1/Taz* causes lethality predominantly in male mice.

During the observation period, we noticed that the weight of *Yap1/Taz$^{i\Delta EC}$* mice was significantly higher than control mice (Fig. 2A and B). The weight difference was more evident in male *Yap1/Taz$^{i\Delta E}$* mice (1.30-fold) compared to female ones (1.07-fold). To clarify the cause of lethality in male *Yap1/Taz$^{i\Delta EC}$* mice, we performed micro-CT imaging (Fig. 2C). *Yap1/Taz$^{i\Delta EC}$* mice showed massive pleural effusion in the thorax and cardiomegaly (average CTR = 0.71 in control and 0.83 in *Yap1/Taz$^{i\Delta EC}$* mice), and these findings were more discernible in males than females (Fig. 2D). To reveal the mechanism underlying the lethal phenotype of male *Yap1/Taz$^{i\Delta EC}$* mice, we examined histology of various tissues. HE staining of tissue sections revealed lung congestion with dilated capillaries in the alveolar walls and mild hepatic congestion with dilated central veins and sinusoids in male *Yap1/Taz$^{i\Delta EC}$* mice (Fig. 2E and Supplementary Fig. S2A), indicating congestion due to circulation failure. Massive subcutaneous edema was observed in the skin of male *Yap1/Taz$^{i\Delta EC}$* mice (Supplementary Fig. S2B). Vascular and lymphatic vessels were dilated in the skin, which might be indicative of increased vascular permeability. Overall, these data indicate that YAP1/TAZ maintain systemic vascular integrity and normal blood circulation predominantly in male mice.

3.2. Endothelial-specific deletion of Yap1/Taz induces systemic circulation failure after irradiation

Vascular integrity is often perturbed by IR-induced tissue injury [1,4], and YAP1/TAZ is reportedly activated upon genotoxic stress [37,38]. Thus, we speculated that endothelial YAP1/TAZ might be critical to maintain vascular integrity upon irradiation. To test if YAP1/TAZ are activated in ECs upon irradiation, we quantified the expression of *Ctgf* and *Cyr61*, two major YAP1/TAZ transcriptional

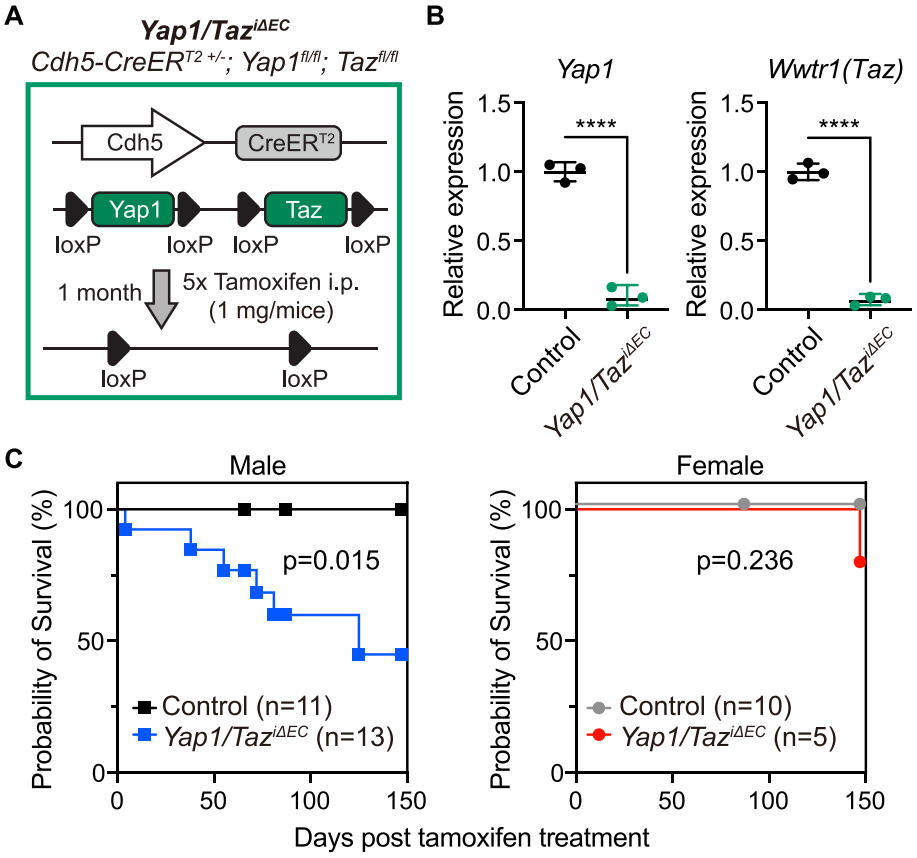

Fig. 1. Endothelial YAP1 and TAZ prevent premature death.
(A) Schematic diagram showing the strategy for conditional deletion of *Yap1/Taz* in vascular ECs. (B) Efficient deletion of *Yap1/Taz* confirmed by quantitative RT-PCR using lung ECs at 4 weeks post-tamoxifen treatment (n = 3). (C) Kaplan-Meier survival curves of control (11 males and 10 females) and *Yap/Taz$^{i\Delta EC}$* (13 males and 5 females) mice after the last injection of tamoxifen.

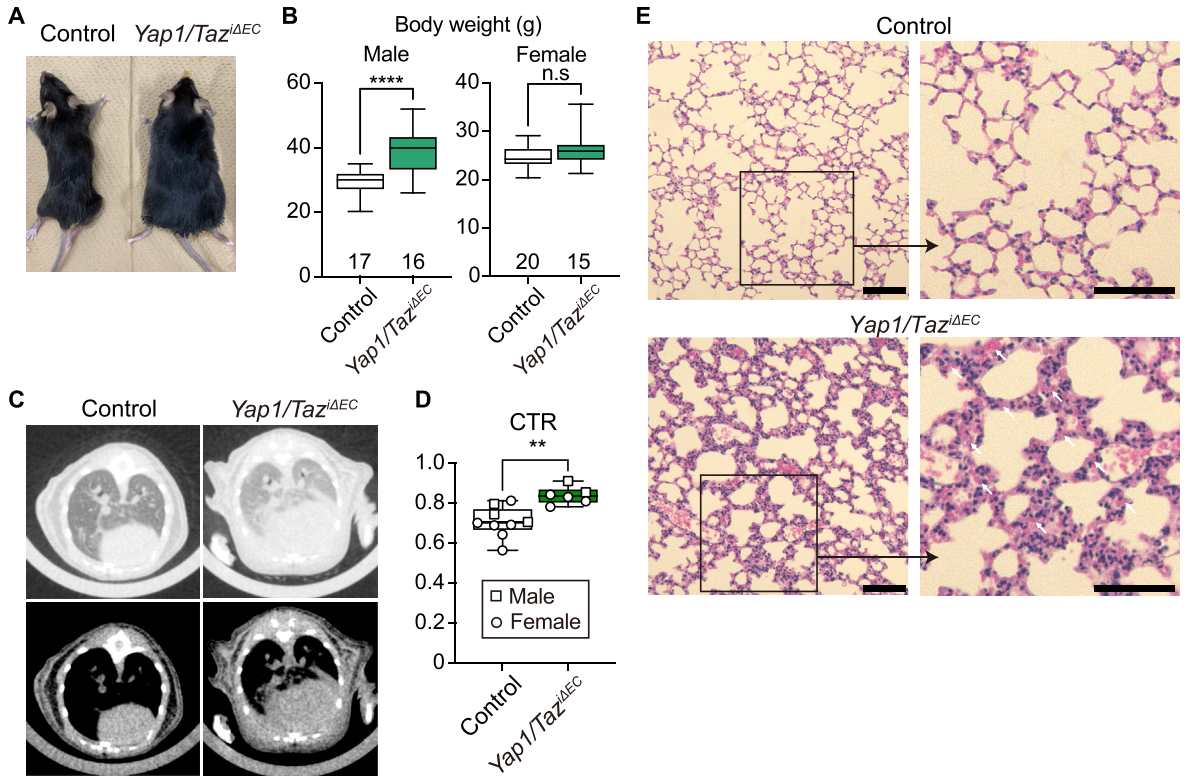

Fig. 2. Endothelial YAP1 and TAZ prevent systemic edema and circulatory failure.
(A) A representative image showing the appearance of male control and *Yap/Taz*$^{i\Delta EC}$ mice. (B) Body weight of control (17 males and 16 females) and *Yap/Taz*$^{i\Delta EC}$ (20 males and 15 females). (C) Representative micro-CT images of male control and *Yap/Taz*$^{i\Delta EC}$ mice. Images with pulmonary window setting (upper) and mediastinal window setting (lower). (D) Cardiothoracic ratio of control (3 males and 6 females) and *Yap/Taz*$^{i\Delta EC}$ (2 males and 4 females) mice in the steady state. (E) HE staining of lung sections obtained from male control and *Yap/Taz*$^{i\Delta EC}$ mice. Arrows indicate dilated capillaries. Bars = 100 μm.

targets [6], in lung ECs before and after sublethal IR. Quantitative RT-PCR revealed that both of the YAP1/TAZ targets were significantly upregulated at 24 h after IR, indicating that YAP1/TAZ were indeed activated in lung ECs upon IR (Fig. 3A). To explore the biological effect of endothelial YAP1/TAZ activation upon IR, we monitored the survival of *Yap1/Taz*$^{i\Delta EC}$ mice after IR (Fig. 3B). Strikingly, while all control mice survived the sublethal IR, all irradiated *Yap1/Taz*$^{i\Delta EC}$ mice died within 10 days regardless of their sex (Fig. 3C).

Moreover, in contrast to the steady-state condition, we observed remarkable weight gain in both male and female *Yap1/Taz*$^{i\Delta EC}$ mice upon IR (Fig. 3D and Supplementary Fig. S3A). Micro-CT analysis revealed massive pleural effusion (Fig. 3E) and cardiomegaly in *Yap1/Taz*$^{i\Delta EC}$ mice post-IR (Supplementary Fig. S3B). Histological analysis of various tissues revealed lung congestion with dilated capillaries in the alveolar walls (Fig. 3F), advanced hepatic congestion with dilated central veins and sinusoids, and massive edema and dilatation of vascular and lymphatic vessels in the skin of *Yap1/Taz*$^{i\Delta EC}$ mice (Supplementary Fig. S2B). Collectively, these results indicate that YAP1/TAZ activation in ECs is critical to prevent IR-induced vascular disruption and thus protects mice from systemic edema, circulation failure, and acute lethality.

3.3. Down-regulation of tight junction-related genes in *Yap1/Taz*$^{i\Delta EC}$ ECs

To investigate the molecular mechanism underlying vascular dysfunction in *Yap1/Taz*$^{i\Delta EC}$ mice, we performed RNA-seq analysis of lung ECs isolated from male control and *Yap1/Taz*$^{i\Delta EC}$ mice. Principal component analysis (PCA) revealed that *Yap1/Taz*$^{i\Delta EC}$ ECs have a distinct transcriptomic profile from control ECs (Fig. 4A). We then identified differentially expressed genes (DEGs) between control and *Yap1/Taz*$^{i\Delta EC}$ ECs using the cutoff value FDR <0.05. In total, 432 and 469 genes were significantly upregulated and downregulated in *Yap1/Taz*$^{i\Delta EC}$ ECs compared with control ECs, respectively (Fig. 4B and Supplementary Table S3). KEGG pathway analysis indicated enrichment of genes involved in the cell cycle in upregulated DEGs and tight junction in downregulated DEGs (Fig. 4C). Gene set enrichment analysis (GSEA) demonstrated that YAP1 signature genes were significantly downregulated in *Yap1/Taz*$^{i\Delta EC}$ (Fig. 4D). We also confirmed that most of the YAP1/TAZ target genes [39] were downregulated in *Yap1/Taz*$^{i\Delta EC}$ ECs (Supplementary Fig. 4A). Moreover, GSEA showed downregulation of tight junction-related genes [40] in *Yap1/Taz*$^{i\Delta EC}$ ECs. Of note, the majority of claudin family genes were significantly downregulated in *Yap1/Taz*$^{i\Delta EC}$ (Supplementary Fig. 4B), suggesting disruption of tight junctions in ECs as the underlying mechanism for increased edema and pleural effusion in *Yap1/Taz*$^{i\Delta EC}$ mice. Together, these data indicate that basal activity of YAP1/TAZ in ECs is critical to maintain expression of multiple claudins, major structural components of tight junctions that regulate vascular integrity.

4. Discussion

Previous studies revealed various functions of YAP1/TAZ in organ development, tissue regeneration, and stress response [6,8,41]. However, it is poorly understood how adult endothelial YAP1/TAZ act during homeostasis and after genotoxic stress. Our current

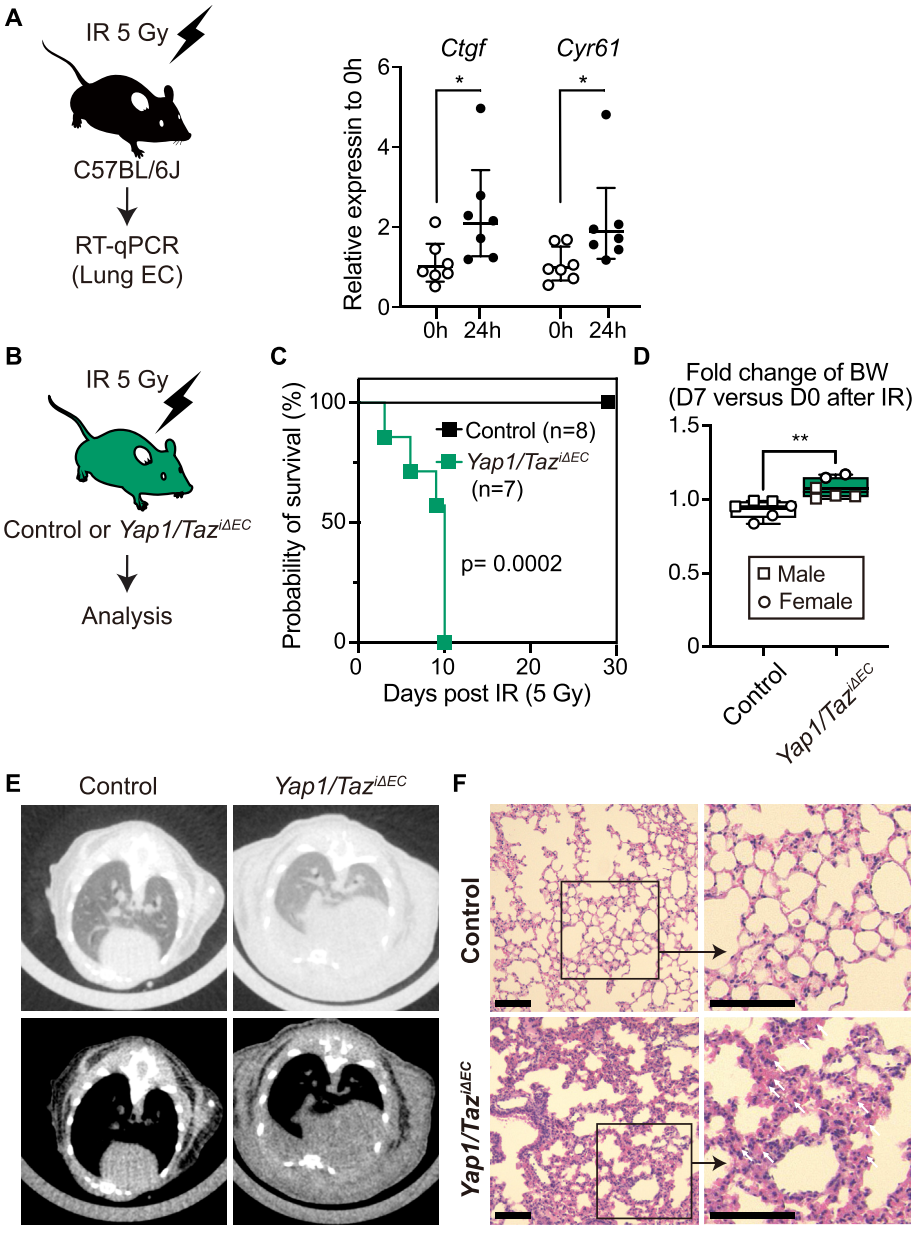

Fig. 3. Irradiation-induced YAP1/TAZ activation is critical for vascular integrity and organismal survival.
(A) Expression levels of YAP1/TAZ target genes in lung ECs before and 24 h after IR. (B) Experimental design for analyzing control and *Yap/Taz*$^{i\Delta EC}$ mice after IR. (C) Kaplan-Meier survival curves of control (5 males and 3 females) and *Yap/Taz*$^{i\Delta EC}$ (5 males and 2 females) mice after 5 Gy IR. (D) IR-induced body weight changes in control (3 males and 3 females) and *Yap/Taz*$^{i\Delta EC}$ mice (4 males and 2 females). (E) Representative micro-CT images of male control and *Yap/Taz*$^{i\Delta EC}$ mice on day 7 after IR. Images with pulmonary window setting (upper) and mediastinal window setting (lower). (F) HE staining of lung sections obtained from male control and *Yap/Taz*$^{i\Delta EC}$ mice on day 7 post-IR. Arrows indicate dilated capillaries. Bars, 100 μm.

study identified sex- and context-dependent roles of YAP1/TAZ in vascular integrity and organismal survival. Our results indicate that basal activity of endothelial YAP1/TAZ is critical to prevent vascular dysfunction, systemic edema, and circulation failure. The discrepancy between this observation and the previous report by Kim et al. [16] could be attributed to sex differences in EC dependency on YAP1/TAZ activity. Neither *Yap1* nor *Taz* is located on sex chromosomes, but emerging evidence suggests that the activity of YAP1/TAZ is differentially regulated by sex hormone receptors [30,31]. In clinical practice, it is well known that male sex is strongly associated with increased risk for cardiovascular disease [42], which could be accounted for at least in part by protective function of estrogens on EC barrier function [30,31,44]. Thus, it is tempting to speculate that male ECs would rely more on basal YAP1/TAZ activity to maintain tight junctions due to low availability of estrogen-mediated vascular protection.

Our results also highlight the importance of endothelial YAP1/TAZ activation upon genotoxic stress. In this context, we did not see sex differences in endothelial YAP1/TAZ function, indicating that YAP1/TAZ counteract IR-induced vascular damage in a sex-independent manner. We previously demonstrated that over-activation of endothelial p53 disrupts vascular integrity [1], and YAP1/TAZ activity may hold p53 activity in check upon IR. Moreover, endothelial YAP1/TAZ are also known to be essential to

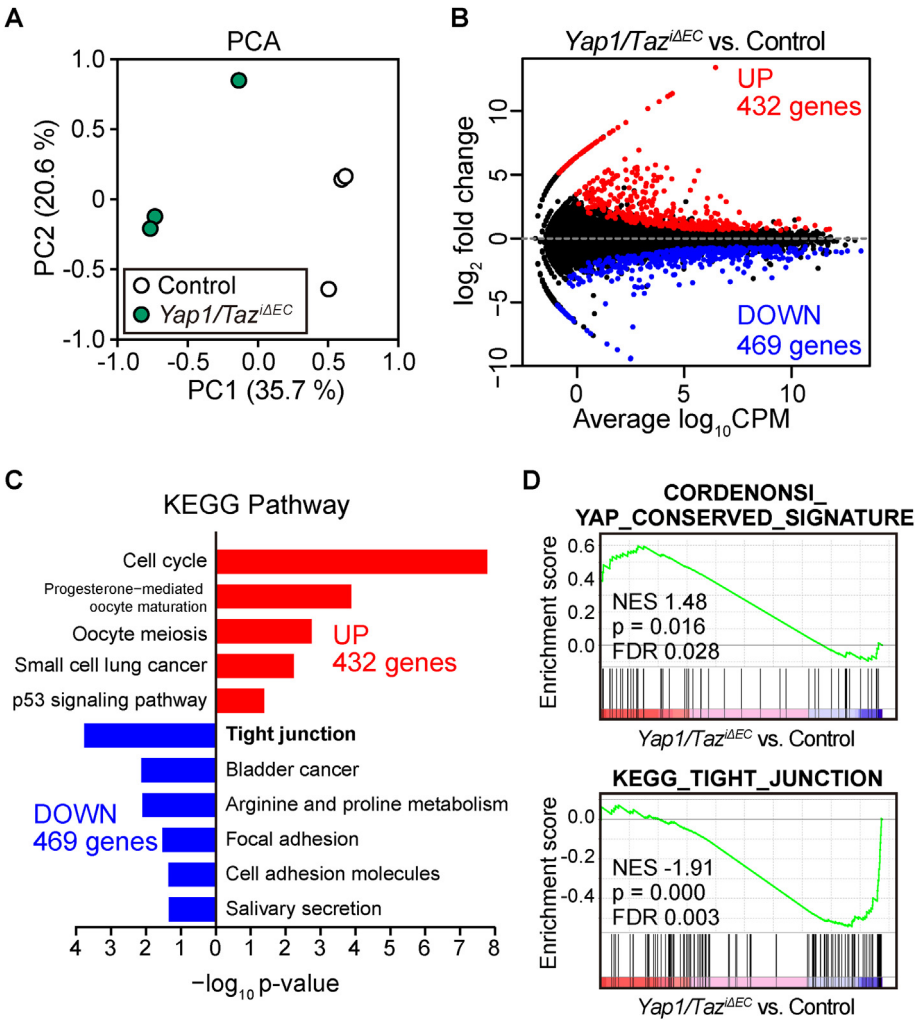

Fig. 4. Expression profiles of ECs that lack YAP1/TAZ.
(A) PCA plot of RNA-seq data obtained from male control and *Yap1/Taz*$^{i\Delta EC}$ ECs. The percentage of variance explained by each principal component is displayed on each axis. (B) MA plot showing average expression (count per million in log: $\log_{10}$ CPM) and $\log_2$ fold changes between control and *Yap1/Taz*$^{i\Delta EC}$ ECs. The red and blue dots represent 432 upregulated (UP) and 469 downregulated (DOWN) DEGs in *Yap1/Taz*$^{i\Delta EC}$ ECs, respectively. (C) KEGG pathways enriched in UP and DOWN DEGs. (D) GSEA plots showing enrichment of *Yap1* signature (upper) and tight junction-related genes (lower).

vascular integrity upon systemic inflammation [43], and this can hold true for IR-induced inflammation.

Our RNA-seq results point to claudin families as the downstream targets of YAP1/TAZ. This supports the notion that the leaky and dilated vasculature and circulation failure observed in *Yap1/Taz*$^{i\Delta EC}$ mice are due to impaired tight junction of ECs. It is well known that the endothelial tight junction serves important functions in vascular permeability, leukocyte extravasation, and angiogenesis [44]. Disruption of cell-cell junctions inactivates Hippo-pathway and stimulates YAP1/TAZ activation [45]. Activated YAP1/TAZ, in turn, directly and indirectly induce the expression of cell-cell junction-related genes. In this manner, YAP1/TAZ and cell-cell junction form a feedforward loop that maintains vascular integrity. Our results highlight the importance of endothelial YAP1/TAZ in maintaining vascular function through upregulation of tight junction genes.

In conclusion, our findings underscore the importance of endothelial YAP1/TAZ for maintaining adult vascular function. Pharmacological activation of YAP1/TAZ may prevent IR-induced vascular injury and provide a clinical benefit in radiation therapy.

Declaration of competing interest

The authors declare that they have no known competing financial interests or personal relationships that could have appeared to influence the work reported in this paper.

Acknowledgements

We thank J. Wrana (Lunenfeld-Tanenbaum Research Institute) and Y. Kubota (Keio University) for *Taz*$^{flox/flox}$ and *Cdh5-CreER*^{T2} mice, respectively. The super-computing resource was provided by The Human Genome Center, The Institute of Medical Science, The University of Tokyo (IMSUT). We also thank T. Ando (Pathology Core Laboratory, IMSUT) for technical support of HE staining. This work was supported in part by Grants-in-Aid for Scientific Research (#19H05653) and Scientific Research on Innovative Area "Replication of Non-Genomic Codes" (#19H05746) from Japan Society for the Promotion of Science (JSPS), Japan, and Moonshot project (#21zf0127003h0001) from AMED, Japan.

Appendix A. Supplementary data

Supplementary data to this article can be found online at https://doi.org/10.1016/j.bbrc.2022.06.050.

References

[1] S. Si, Y. Nakajima-Takagi, T. Iga, et al., Hematopoietic insults damage bone marrow niche by activating p53 in vascular endothelial cells, Exp. Hematol. 63 (2018) 41–51, https://doi.org/10.1016/j.exphem.2018.04.006, e1.

[2] H. Wijerathne, J. Langston, Q. Yang, et al., Mechanisms of radiation-induced endothelium damage: emerging models and technologies, Radiother. Oncol. 158 (2021) 21–32, https://doi.org/10.1016/j.radonc.2021.02.007.

[3] M.P. Little, L.B. Zablotska, S.E. Lipshultz, Ischemic heart disease after breast cancer radiotherapy, N. Engl. J. Med. 368 (2013) 2523–2527, https://doi.org/10.1056/nejmc1304601.

[4] B. Baselet, P. Sonveaux, S. Baatout, et al., Pathological effects of ionizing radiation: endothelial activation and dysfunction, Cell. Mol. Life Sci. 76 (2019) 699–728, https://doi.org/10.1007/s00018-018-2956-z.

[5] Y. Shimizu, K. Kodama, N. Nishi, et al., Radiation exposure and circulatory disease risk: hiroshima and Nagasaki atomic bomb survivor data, 1950-2003, BMJ 340 (2010), b5349, https://doi.org/10.1136/bmj.b5349.

[6] I.M. Moya, G. Halder, Hippo–YAP/TAZ signalling in organ regeneration and regenerative medicine, Nat. Rev. Mol. Cell Biol. 20 (2018) 1, https://doi.org/10.1038/s41580-018-0086-y.

[7] J.O. Russell, F.D. Camargo, Hippo signalling in the liver: role in development, regeneration and disease, Nat Rev Gastroentero (2022) 1–16, https://doi.org/10.1038/s41575-021-00571-w.

[8] F.-X.X. Yu, B. Zhao, K.-L.L. Guan, Hippo pathway in organ size control, tissue homeostasis, and cancer, Cell 163 (2015) 811–828, https://doi.org/10.1016/j.cell.2015.10.044.

[9] Y. Xiao, M.C. Hill, M. Zhang, et al., Hippo signaling plays an essential role in cell state transitions during cardiac fibroblast development, Dev. Cell 45 (2018) 153–169, https://doi.org/10.1016/j.devcel.2018.03.019, e6.

[10] F. Calvo, N. Ege, A. Grande-Garcia, et al., Mechanotransduction and YAP-dependent matrix remodelling is required for the generation and maintenance of cancer-associated fibroblasts, Nat. Cell Biol. 15 (2013) 637–646, https://doi.org/10.1038/ncb2756.

[11] R. Johnson, G. Halder, The two faces of Hippo: targeting the Hippo pathway for regenerative medicine and cancer treatment, Nat. Rev. Drug Discov. 13 (2013), nrd4161, https://doi.org/10.1038/nrd4161.

[12] F. Zanconato, M. Cordenonsi, S. Piccolo, Yap, TAZ, A signalling hub of the tumour microenvironment, Nat. Rev. Cancer (2019) 1–11, https://doi.org/10.1038/s41568-019-0168-y.

[13] C.D.K. Nguyen, C. Yi, YAP/TAZ signaling and resistance to cancer therapy, Trends Cancer 5 (2019) 283–296, https://doi.org/10.1016/j.trecan.2019.02.010.

[14] A. Hooglugt, M.M. van der Stoel, R.A. Boon, et al., Endothelial YAP/TAZ signaling in angiogenesis and tumor vasculature, Front. Oncol. 10 (2021), 612802, https://doi.org/10.3389/fonc.2020.612802.

[15] X. Wang, A.F. Valls, G. Schermann, et al., YAP/TAZ orchestrate VEGF signaling during developmental angiogenesis, Dev. Cell 42 (2017) 462–478, https://doi.org/10.1016/j.devcel.2017.08.002, e7.

[16] J. Kim, Y.H. Kim, J. Kim, et al., YAP/TAZ regulates sprouting angiogenesis and vascular barrier maturation, J. Clin. Invest. 127 (2017) 3441–3461, https://doi.org/10.1172/jci93825.

[17] J. He, Q. Bao, Y. Zhang, et al., Yes-associated protein promotes angiogenesis via signal transducer and activator of transcription 3 in endothelial cells, Circ. Res. 122 (2018) 591–605, https://doi.org/10.1161/circresaha.117.311950.

[18] H.-J. Choi, H. Zhang, H. Park, et al., Yes-associated protein regulates endothelial cell contact-mediated expression of angiopoietin-2, Nat. Commun. 6 (2015) 6943, https://doi.org/10.1038/ncomms7943.

[19] Y. Shen, X. Wang, Y. Liu, et al., STAT3-YAP/TAZ signaling in endothelial cells promotes tumor angiogenesis, Sci. Signal. 14 (2021), eabj8393, https://doi.org/10.1126/scisignal.abj8393.

[20] T. Mammoto, M. Muyleart, A. Mammoto, Endothelial YAP1 in regenerative lung growth through the angiopoietin–tie2 pathway, Am J Resp Cell Mol 60 (2018) 117–127, https://doi.org/10.1165/rcmb.2018-0105oc.

[21] A.L. Elaimy, A.M. Mercurio, Convergence of VEGF and YAP/TAZ signaling: implications for angiogenesis and cancer biology, Sci. Signal. 11 (2018), eaau1165, https://doi.org/10.1126/scisignal.aau1165.

[22] K.K. Sivaraj, B. Dharmalingam, V. Mohanakrishnan, et al., YAP1 and TAZ negatively control bone angiogenesis by limiting hypoxia-inducible factor signaling in endothelial cells, Elife 9 (2020), e50770, https://doi.org/10.7554/elife.50770.

[23] M. Sakabe, J. Fan, Y. Odaka, et al., YAP/TAZ-CDC42 signaling regulates vascular tip cell migration, Proc. Natl. Acad. Sci. USA 114 (2017) 10918–10923, https://doi.org/10.1073/pnas.1704030114.

[24] A. Totaro, M. Castellan, D.D. Biagio, et al., Crosstalk between YAP/TAZ and notch signaling, Trends Cell Biol. 28 (2018) 560–573, https://doi.org/10.1016/j.tcb.2018.03.001.

[25] A. Totaro, M. Castellan, G. Battilana, et al., YAP/TAZ link cell mechanics to Notch signalling to control epidermal stem cell fate, Nat. Commun. 8 (2017), 15206, https://doi.org/10.1038/ncomms15206.

[26] D. Yasuda, D. Kobayashi, N. Akahoshi, et al., Lysophosphatidic acid-induced YAP/TAZ activation promotes developmental angiogenesis by repressing Notch ligand Dll4, J. Clin. Invest. 129 (2019) 4332–4349, https://doi.org/10.1172/jci121955.

[27] G. Hao, T. Lv, Y. Wu, et al., The Hippo signaling pathway: a potential therapeutic target is reversed by a Chinese patent drug in rats with diabetic retinopathy, Bmc Complem Altern M 17 (2017) 187, https://doi.org/10.1186/s12906-017-1678-3.

[28] J. Um, J. Yu, K.-S. Park, Substance P accelerates wound healing in type 2 diabetic mice through endothelial progenitor cell mobilization and Yes-associated protein activation, Mol. Med. Rep. 15 (2017) 3035–3040, https://doi.org/10.3892/mmr.2017.6344.

[29] T. Azad, M. Ghahremani, X. Yang, The role of YAP and TAZ in angiogenesis and vascular mimicry, Cells 8 (2019) 407, https://doi.org/10.3390/cells8050407.

[30] X. Zhou, S. Wang, Z. Wang, et al., Estrogen regulates Hippo signaling via GPER in breast cancer, J. Clin. Invest. 125 (2015) 2123–2135, https://doi.org/10.1172/jci79573.

[31] G. Kuser-Abali, A. Alptekin, M. Lewis, et al., YAP1 and AR interactions contribute to the switch from androgen-dependent to castration-resistant growth in prostate cancer, Nat. Commun. 6 (2015) 8126, https://doi.org/10.1038/ncomms9126.

[32] H. Omori, M. Nishio, M. Masuda, et al., YAP1 is a potent driver of the onset and progression of oral squamous cell carcinoma, Sci. Adv. 6 (2020), eaay3324, https://doi.org/10.1126/sciadv.aay3324.

[33] K. Okabe, S. Kobayashi, T. Yamada, et al., Neurons limit angiogenesis by titrating VEGF in retina, Cell 159 (2014) 584–596, https://doi.org/10.1016/j.cell.2014.09.025.

[34] A. Subramanian, P. Tamayo, V.K. Mootha, et al., Gene set enrichment analysis: a knowledge-based approach for interpreting genome-wide expression profiles, Proc. Natl. Acad. Sci. USA 102 (2005) 15545–15550, https://doi.org/10.1073/pnas.0506580102.

[35] M. Cordenonsi, F. Zanconato, L. Azzolin, et al., The Hippo transducer TAZ confers cancer stem cell-related traits on breast cancer cells, Cell 147 (2011) 759–772, https://doi.org/10.1016/j.cell.2011.09.048.

[36] D.J. McCarthy, Y. Chen, G.K. Smyth, Differential expression analysis of multifactor RNA-Seq experiments with respect to biological variation, Nucleic Acids Res. 40 (2012) 4288–4297, https://doi.org/10.1093/nar/gks042.

[37] Y. Zhang, Y. Wang, D. Zhou, et al., Radiation-induced YAP activation confers glioma radioresistance via promoting FGF2 transcription and DNA damage repair, Oncogene 40 (2021) 4580–4591, https://doi.org/10.1038/s41388-021-01878-3.

[38] A. Gregorieff, Y. Liu, M.R. Inanlou, et al., Yap-dependent reprogramming of Lgr5+ stem cells drives intestinal regeneration and cancer, Nature 526 (2015) 715–718, https://doi.org/10.1038/nature15382.

[39] Y. Wang, X. Xu, D. Maglic, et al., Comprehensive molecular characterization of the Hippo signaling pathway in cancer, Cell Rep. 25 (2018) 1304–1317, https://doi.org/10.1016/j.celrep.2018.10.001, e5.

[40] C. Zihni, C. Mills, K. Matter, et al., Tight junctions: from simple barriers to multifunctional molecular gates, Nat. Rev. Mol. Cell Biol. 17 (2016) 564–580, https://doi.org/10.1038/nrm.2016.80.

[41] T. Panciera, L. Azzolin, M. Cordenonsi, et al., Mechanobiology of YAP and TAZ in physiology and disease, Nat. Rev. Mol. Cell Biol. 18 (2017) 758–770, https://doi.org/10.1038/nrm.2017.87.

[42] L. Mosca, E. Barrett-Connor, N.K. Wenger, Sex/gender differences in cardiovascular disease prevention, Circulation 124 (2011) 2145–2154, https://doi.org/10.1161/circulationaha.110.968792.

[43] Y. Lv, K. Kim, Y. Sheng, et al., YAP controls endothelial activation and vascular inflammation through TRAF6, Circ. Res. 123 (2018) 43–56, https://doi.org/10.1161/circresaha.118.313143.

[44] Y. Wallez, P. Huber, Endothelial adherens and tight junctions in vascular homeostasis, inflammation and angiogenesis, Biochimica Et Biophysica Acta Bba - Biomembr 1778 (2008) 794–809, https://doi.org/10.1016/j.bbamem.2007.09.003.

[45] R. Karaman, G. Halder, Cell junctions in Hippo signaling, Csh Perspect Biol 10 (2018), a028753, https://doi.org/10.1101/cshperspect.a028753.

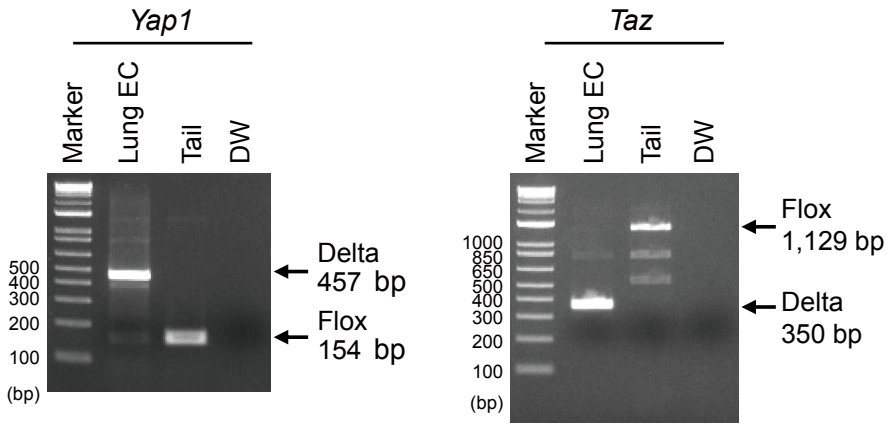

Supplementary Fig. 1. Efficient EC-specific deletion of *Yap1/Taz*

EC-specific deletion of *Yap1/Taz* confirmed by genomic PCR using lung EC and tail DNA. DW, distilled water.

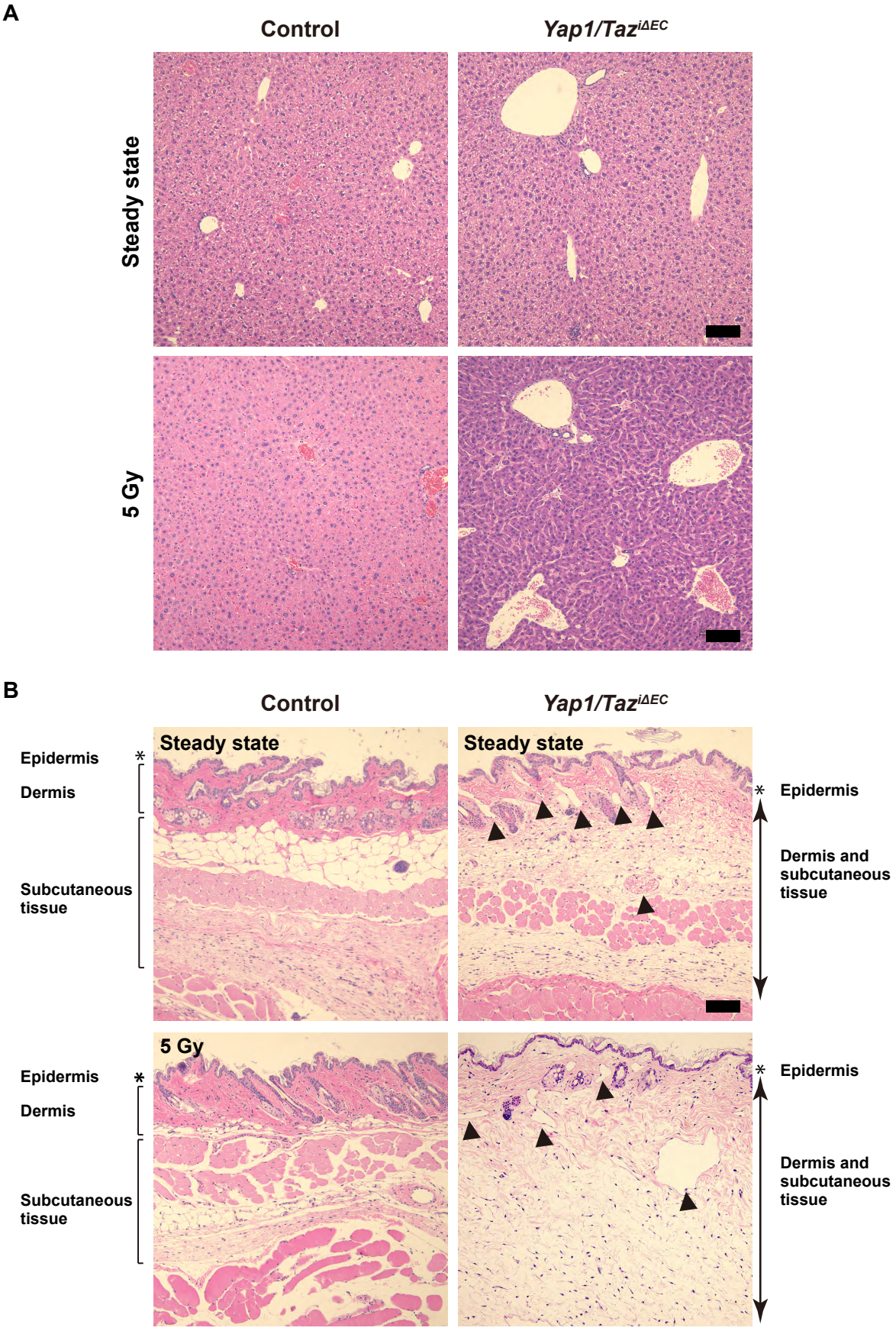

Supplementary Fig. 2. Endothelial *Yap1/Taz* deletion causes hepatic congestion and skin edema. HE staining of liver (A) and skin (B) sections obtained from male control and *Yap/Taz*$^{i\Delta EC}$ mice. Arrow heads indicate dilated vascular or lymphatic vessels. Bars = 100 μm

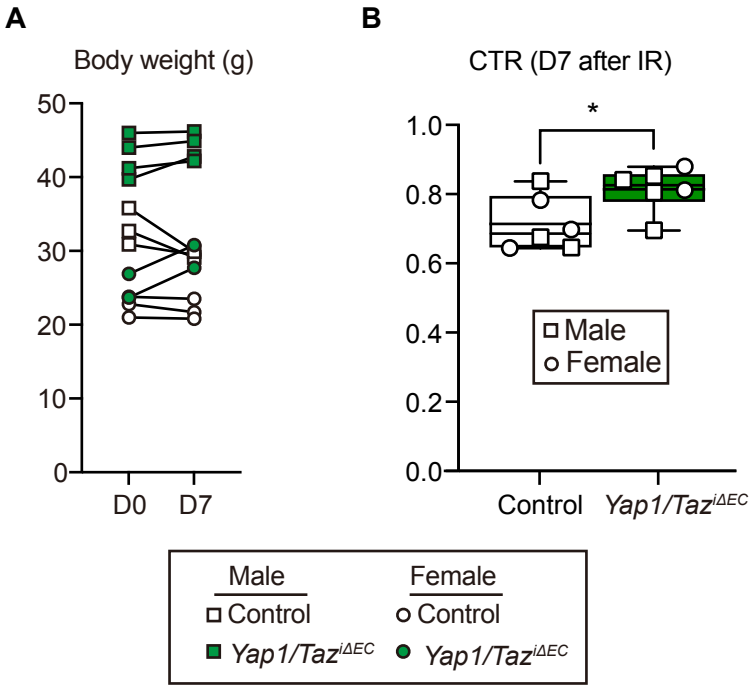

Supplementary Fig. 3. Irradiation causes body weight gain and cardiac enlargement in *Yap/Taz$^{i\Delta EC}$* mice
Body weight (A) and CTR (B) of control (n=3 males and 3 females) and Yap/TaziΔEC (n=4 males and 2 females) mice before (D0) and/or 7 days after IR (D7).

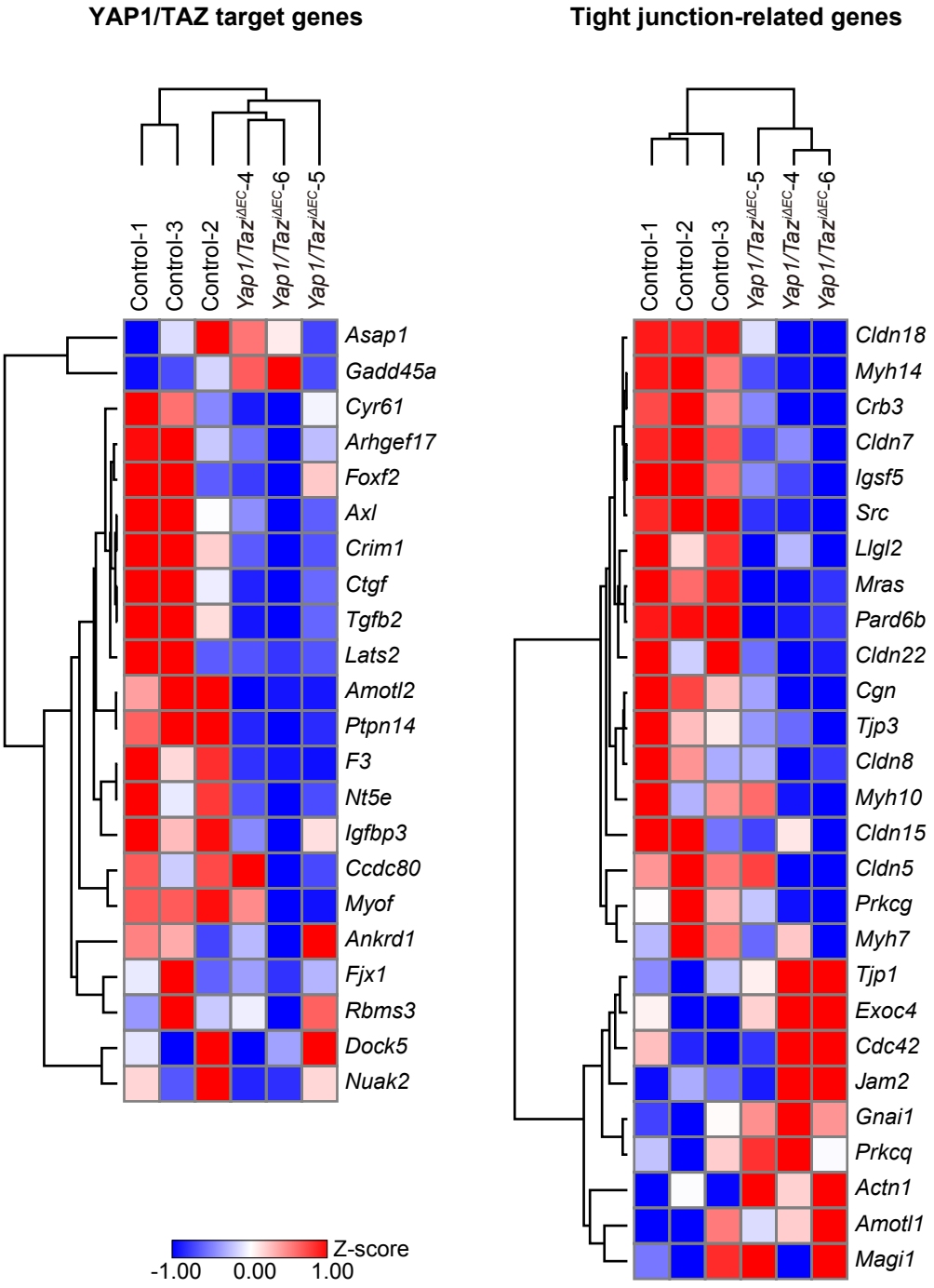

Supplementary Fig. 4. Reduced expression of Yap1/Taz target genes and tight junction-related genes in *Yap/Taz*$^{i\Delta EC}$ ECs

Heatmap showing Z-score of TPM for YAP1/TAZ target genes (left) and tight junction-related genes (right) in control (n=3) and *Yap/Taz*$^{i\Delta EC}$ (n=3) ECs. The color code indicates high (red) and low (blue) expression levels.